

# CO adsorption on close-packed transition and noble metal surfaces: Trends from ab-initio calculations

Marek Gajdoš,\* Andreas Eichler, and Jürgen Hafner  
*Institut für Materialphysik and Center for Computational Materials Science  
Universität Wien, Sensengasse 8/12, A-1090 Wien, Austria*

(Dated: November 26, 2024)

We have studied the trends in CO adsorption on close-packed metal surfaces: Co, Ni, Cu from the 3d row, Ru, Rh, Pd, Ag from the 4d row and Ir, Pt, Au from the 5d row using density functional theory. In particular, we were concerned with the trends in the adsorption energy, the geometry, the vibrational properties and other parameters derived from the electronic structure of the substrate. The influence of specific changes in our setup such as choice of the exchange correlation functional, the choice of pseudopotential and size of the basis set, substrate relaxation has been carefully evaluated. We found that while the geometrical and vibrational properties of the adsorbate-substrate complex are calculated with high accuracy, the adsorption energies calculated with the gradient-corrected Perdew-Wang exchange-correlation energies are overestimated. In addition, the calculations tend to favour adsorption sites with higher coordination, resulting in the prediction of wrong adsorption sites for the Rh, Pt and Cu surfaces (hollow instead of top). The revised Perdew-Burke-Erzerhof functional (RPBE) leads to lower (i.e. more realistic) adsorption energies for transition metals, but to wrong results for noble metals - for Ag and Au endothermic adsorption is predicted. The site preference remains the same. We discuss trends in relation to the electronic structure of the substrate across the Periodic Table, summarizing the state-of-the-art of CO adsorption on close-packed metal surfaces.

PACS numbers:

## I. INTRODUCTION

The development of modern theoretical surface science provides an opportunity to investigate surfaces and adsorbate structures on the atomic scale with useful applications in industrial technologies. Much effort has been devoted to study CO chemisorption and dissociation on transition metals. There are numerous papers and reviews which deal with this system from different points of view (electronic, structural, vibrational) [1, 2, 3, 4]. One of the central questions is how the strength of the chemisorption of CO and the preference for the specific adsorption site varies across the transition metal (TM) series. A particular case, CO adsorption on the Pt(111) surface, has attracted much attention in the past, since for this system state-of-the-art DFT calculations fail in predicting the correct site preference [5]. The question which immediately arises, whether this case is an exception or the rule?

Additionally, a vast number of theoretical papers appeared in the literature since Ying, Smith and Kohn presented in the mid 70's a first self-consistent density functional study of chemisorption on metal surfaces (H on tungsten) [6]. The number of theoretical adsorption studies of TM molecules on different surfaces is increasing with time not only because of their importance in catalysis, but also due to the increasing reliability of the "measured" properties. In the past, several systematic

studies of the adsorption of CO molecules on transition metal surfaces have been performed [2, 7, 8, 9]. In 1990 Nørskov proposed a model of chemisorption on transition metal surfaces which was later expanded and is now quite generally accepted [8, 9]. A main feature of the model is the importance of the position of the d-band center relative to the HOMO and LUMO of the adsorbate. The importance of understanding the correlation between the geometric and the electronic structure arises from the proposed mechanistic model for chemisorption. One among several trends is the correlation between the CO stretching frequency  $\nu_{C-O}$  and the energy level difference between  $5\sigma$  and  $1\pi$  orbitals of the adsorbed CO ( $\Delta(5\sigma - 1\pi)$ ) proposed by Ishi et al. [10].

In this paper we present an extensive density functional study of the adsorption of CO on the closed-packed surfaces [(111) for face-centered cubic, resp. (0001) for hexagonal metals] of Co, Ni, Cu, Ru, Rh, Pd, Ag, Ir, Pt and Au. After a description of the set-up in Section II, we characterize briefly the clean surfaces in Section III. Section IV is devoted to the adsorption of CO. Starting from the geometric structure of the adsorbate-substrate system, going through vibrational and electronic properties (stretching frequencies of the adsorbate, and of the adsorbate-substrate bond, occupation of the anti-bonding  $2\pi^*$ -like orbital, density of states, redistribution of the charge density) as well as site preference we draw a complete picture of the CO adsorption on the close-packed TM surfaces. Moreover, we investigate the influence of the exchange-correlation functional and the cut-off energy on the site preference (Section V). In Section VI we discuss our results in the light of the experimental literature and analyze trends and correlations between

---

\*Electronic address: Marek.Gajdos@univie.ac.at

the investigated properties. This paper tries to go beyond a pure table of references from experiments and different DFT calculations, by providing a large and consistent database, in which each element was treated in exactly the same manner. Further, one of our main goals is not only to obtain theoretical values of spectroscopic accuracy, but also to derive useful trends of CO adsorption on 3d, 4d and 5d transition metal surfaces with the hope of applicability in the prediction of the adsorption and catalytic behavior.

## II. METHODOLOGY

The calculations in this work are performed using the Vienna ab-initio simulation package VASP [11, 12] which is a DFT code, working in a plane-wave basis set. The electron-ion interaction is described using the projector-augmented-wave (PAW) method [13, 14] with plane waves up to an energy of  $E_{\text{cut}} = 450$  eV (for some calculations harder pseudopotentials were used for C and O which require energy cut-off of 700 eV). For exchange and correlation the functional proposed by Perdew and Zunger [15] is used, adding (semi-local) generalized gradient corrections (GGA) of various flavor (PW91 [16], RPBE [17]). These GGAs represent a great improvement over the local density approximation (LDA) in the description of the adsorption process.

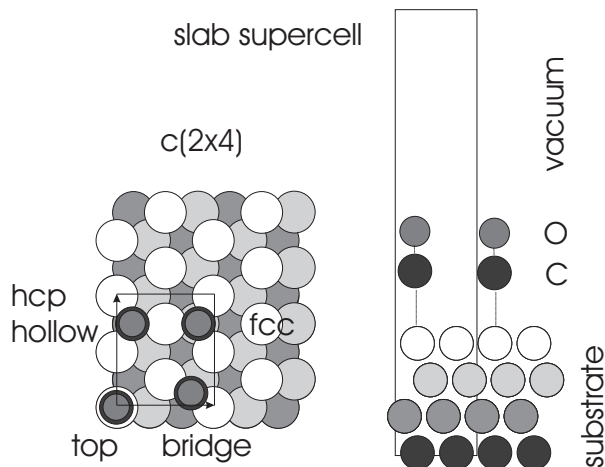


FIG. 1: Top and side view of the slab used in the calculations. In the top view of the  $c(2 \times 4)$  cell we denote all investigated high-symmetry sites.

The substrate is modelled by four layers of metal separated by a vacuum layer of approximately double thickness, as shown in Fig. 1. The two uppermost substrate layers and the CO molecule are allowed to relax. This enables us to check the influence of the relaxation on the adsorption system. The Brillouin zone of the  $c(2 \times 4)$  surface cell (equivalent to a coverage of  $\Theta = 0.25$  ML) was

sampled by a grid of  $(4 \times 3 \times 1)$  k-points. We have chosen this coverage as a compromise between small adsorbate-adsorbate interactions (“low coverage limit”) and low computational effort.

In the calculation we investigated the adsorption on the close packed surfaces of 10 metallic elements from the 3d (Co, Ni, Cu), 4d (Ru, Rh, Pd, Ag) and 5d transition metal rows (Ir, Pt, Au) of the Periodic Table. For all hcp-elements, Co and Ru, the (0001) surface was used with the ideal  $c/a$  ratio of 1.63. The spin-polarization of Ni and Co was also taken into account.

Vibrational properties of CO were computed by applying a finite-differences method to create the Hessian matrix which we diagonalize to obtain the characteristic frequencies. We have calculated the metal-CO ( $\nu_{\text{M-CO}}$ ) and C-O stretch ( $\nu_{\text{C-O}}$ ) frequencies in the direction perpendicular to the surface plane.

The free CO molecule is characterized by a calculated stretch frequency of  $2136 \text{ cm}^{-1}$  at an equilibrium bond length of  $1.142 \text{ \AA}$ . The corresponding experimental values are  $2145 \text{ cm}^{-1}$  and  $1.128 \text{ \AA}$  [18]. The problem of a too large CO binding energy ( $E_{\text{CO}}^{\text{PW91}} = 11.76 \text{ eV}$ ,  $E_{\text{CO}}^{\text{exp}} = 11.45 \text{ eV}$  [19]) stems mainly from the error in the energy of the free atom, where high density gradients make an accurate description more difficult.

Further, the bonding of adsorbate to the surface by calculating density of states and charge density flow was investigated.

## III. BULK AND CLEAN SURFACES

### A. Lattice constant

For a general understanding of the adsorption process, especially for the adsorption in higher coordinated sites, the lattice constant of the substrate is an important parameter. The optimal adsorption height for example will always be determined by an interplay between the optimal carbon-metal bond-length and the lattice parameter. For that reason, we give in Fig. 2 the theoretical lattice constants together with the experimental values [20]. These lattice parameters are compared with lattice parameters calculated with the PW91 and RPBE exchange correlation functional.

The overestimation of the lattice parameter (calculated within the GGA) is characteristic for the heavier elements. The difference between the experimental and calculated lattice constant is around 1% for 3-d row metals and around 2% for other elements. Such a 2% difference in the lattice constant corresponds to a change in the CO adsorption energy of about  $0.03 \text{ eV}$  for Pd(100) [21] and Ru(0001) surface [22]. In general, the lattice parameter increases along the rows and columns of the Periodic Table. For a greater lattice constant one might expect that the adsorbate will come closer to the surface. On the other hand, as the width of the d-band increases, the binding is reduced and the actual height of the adsorbate

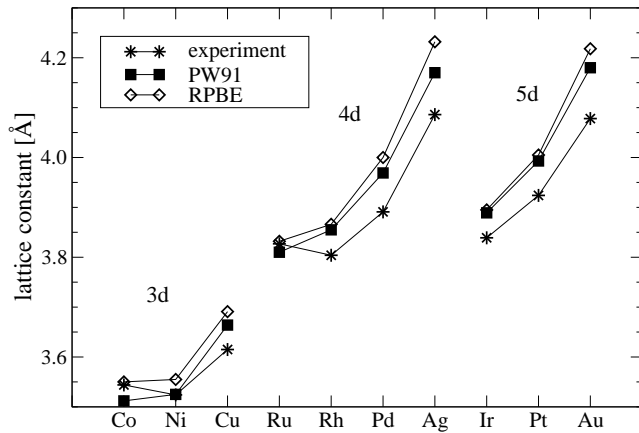


FIG. 2: Lattice parameters for a part of the Periodic Table. We show the experimental and calculated lattice parameters for PW91 and RPBE functional. Although, Ru and Co are hcp metals we have included them together with fcc metals at an ideal  $c/a \doteq 1.63$ .

over the surface should increase.

### B. Work-function

In Fig. 3 we present the calculated work-functions together with experimental values.

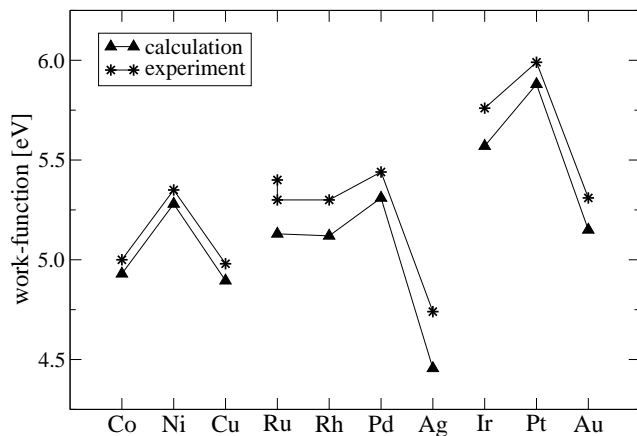


FIG. 3: Experimental and calculated values of the work-function (PW91) for various transition metal (111) surfaces. References for experiments: Co [23], Ni [23], Cu [23], Ru [24, 25], Rh [26], Pd [27], Ag [23], Ir [23], Pt [26, 28], Au [23].

We find that the calculated work-functions (PW91) are in all cases slightly lower (by at most 6% for Ag) than the measured values. The largest discrepancies in terms of absolute values are found for 4d metals, where the differences for Ru, Rh and Ag surface are  $\approx 0.3$  eV. However, in general the agreement is quite good. The work-function

always increases with the d-band filling. Only for the noble metals (Cu, Ag, Au) it decreases again. Similarly, the work-function increases along the columns when going down from the 3d to the 5d metals.

### C. Electronic structure : d-band center

The position of the d-band center of the clean surface is another important characteristic which is closely related to the strength of the CO-surface interaction. As it was already argued [8, 29, 30], the d-band centers play a significant role in the bonding for many adsorbate-substrate systems where the major interaction is due to hybridization of the HOMO and LUMO of the adsorbate and the d-orbitals of the substrate.

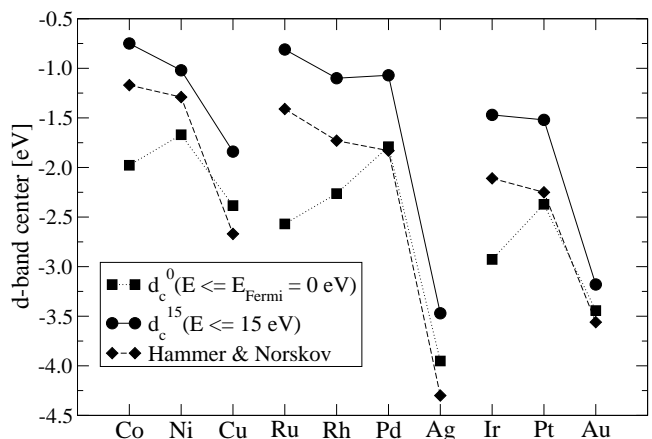


FIG. 4: The d-band centers of the clean TM surfaces integrated until  $E_{\text{Fermi}}$  level and 15 eV above  $E_{\text{Fermi}}$ , where at least 9.5 electrons are accommodated in the d-band. As a comparison the calculated d-band centers from the article of Hammer and Nørskov are taken [8].

However, simple as it might seem to be, the proper definition of the d-band center is not that straightforward:

(i) Within a plane-wave method, partial angular-momentum decomposed densities of states can be defined in different ways. We chose the projection of the plane-wave components onto spherical orbitals within some atomic radius.

(ii) DFT applies only to the ground-state, excited states are usually predicted at too low energies. Therefore we report in Fig. 4 the center of gravity of the occupied d-band (integration up to the Fermi-level)  $d_c^0$ , and the center of the entire d-band  $d_c^{15}$  (integration from the lower band edge up to 15 eV above  $E_{\text{Fermi}}$  where at least 9.5 electrons have been accommodated in the d-band), together with the d-band centers taken from the older LMTO calculations of Hammer and Nørskov ( $d_c^{HN}$ ) [8]. The  $d_c^0$  and  $d_c^{15}$  values provide upper and lower bounds for our d-band centers. The  $d_c^{HN}$  lies in between for TM surfaces, but it is lower in energy for noble metals. This

stems from a small contributions to the density of states far from the main d-band peak. As per definition, the difference between  $d_c^0$  and  $d_c^{15}$  increases with decreasing band-filling.  $d_c^{15}$  shows only little variation in groups VIII to IB. As expected, it drops significantly for the noble metals compared to the metals in the same row.

#### IV. CO ADSORPTION

We have studied the adsorption of CO in the top, bridge and hollow (fcc, hcp) sites in the  $c(2 \times 4)$  cell, corresponding to a coverage of a quarter of a monolayer ( $\Theta=0.25$  ML) (see Fig. 1). From these calculations we derive in the following trends in the adsorption energies, the vibrational properties, the geometric and the electronic structure.

##### A. Adsorption energy and site preference

Beside the adsorption geometry and the vibrational properties a precise determination of the adsorption energy for a given geometry is one of the keys to understanding the mechanism of the catalytical activity and selectivity [31]. The adsorption energy describes the strength of the chemical bond between the CO molecule and the metallic surface.

The adsorption energy for the stable adsorption site corresponds to the absolute minimum on the potential energy surface (PES) of the molecule moving on the surface. The adsorption energies calculated for other high-symmetry sites correspond either to local extreme or to a saddle point on the PES. The position and the height of the saddle points define the diffusion path and the activation energy for surface diffusion.

The experimental isosteric heat of the adsorption  $H_{\text{ads}}(\Theta)$  is not directly comparable with the calculated adsorption energy. If we want to compare our theoretically calculated adsorption energy  $E_{\text{ads}}$  (i.e. the gain in energy when a certain amount of CO is adsorbed) at  $\Theta=0.25$  ML with the isosteric heat of adsorption (a differential energy gained when adsorbing one additional molecule on a surface at a certain CO coverage) we need to take the integral up to the coverage used in the calculation:

$$H_{\text{ads,int}}(\Theta_{\text{calc}}) = \frac{1}{\Theta_{\text{calc}}} \int_0^{\Theta_{\text{calc}}} H_{\text{ads}}(\Theta) d\Theta. \quad (1)$$

The experimental heats of adsorption with and the proposed adsorption sites are presented in Table I. We show adsorption sites which are found at 0.25 ML or up to 0.5 ML coverage.

The main trends in the experimental results given in Table I include:

1. CO adsorption on TM surfaces is several times stronger ( $E_{\text{ads}} \sim 1.2$  to  $1.7$  eV) than on noble metals ( $E_{\text{ads}} \sim 0.3$  to  $0.5$  eV).
2. All measured adsorption sites (with the exception of on-top site on Ru(0001)) show a slight decrease of the heat of adsorption going from the zero coverage limit to a quarter-monolayer coverage.
3. The heat of adsorption decreases with increasing filling of the d-band.

Fig. 5 summarizes the calculated adsorption energies (using the PW91 GGA) for the high symmetry positions described in Fig. 1. For the transition metals we note a pronounced tendency to overestimate the adsorption energies - this is independent of an eventual relaxation of the surface. For the noble metals (with the exception of Cu) on the other hand, the calculations rather tend to underestimate the adsorption energies - this could be related to the neglect of dispersion forces.

Experimentally, the adsorption energies on the TM surfaces are found to decrease monotonously with increasing band filling. In the calculation, the variation depends on the adsorption site:  $E_{\text{ads}}$  decreases for on-top adsorption, but increases for sites with higher coordination. This leads to wrong predictions for Cu, Rh and Pt where the hollow sites were found to be preferred for CO adsorption, whereas experiment shows that adsorption occurs on the top sites. Moreover, the relaxation of the metallic substrate is necessary for Co and Ru surfaces, i.e. if the surface is not allowed to relax we get a different site prediction compared to the experiments. However, even after substrate relaxation, the energies for CO adsorption in hollow and top sites on Co, Ag, and Au surfaces remain almost degenerate. Site preference is indeed a fundamental problem for CO adsorption on metallic surfaces. We shall try to elucidate the origin of this problem below.

Another interesting point is that among the hollow sites, the preference changes from hcp (Co, Ni, Ru, Rh, Ir) to fcc (Cu, Pd, Ag, Pt, Au) with increasing d-band filling.

##### B. Geometric structure

In the past many studies have demonstrated that on the basis of DFT a reliable determination of the geometrical structure is possible. The local adsorption geometry of the CO molecule on an unrelaxed TM surface can uniquely be characterized by the S(urface)-C distance (height above the surface) and the C-O bond length. If additionally the metal atoms are allowed to relax, this modification of the surface can be described by the change of the inter-layer distance and the buckling of the surface.

On all studied surfaces the CO molecule adsorbs in an upright position with the carbon atom pointing towards

		Experiment			Theory					
surface	site	$H_{\text{ads}}(0\text{ML})$	$H_{\text{ads}}(\frac{1}{4}\text{ML})$	$H_{\text{ads,int}}$	method	$\Theta$ [ML]	ref.	$E_{\text{ads}}^{PW91,450}$	$E_{\text{ads}}^{PW91,700}$	$E_{\text{ads}}^{RPBE,700}$
Co	top	-1.33	-1.33	-1.33	SP	0.33	[32]	-1.65	-1.62	-1.32
		-1.19			TDS		[33]			
Ni	hollow	-1.35	-1.28	-1.32	CAL	0.25	[34]	-1.95	-1.90	-1.44
		-1.31	-1.28	-1.30	TDS	0.25	[35]			
		-1.31	-1.06		TDS	0.25	[36]			
Cu	top	-0.49			TDS		[37]	-0.75	-0.72	-0.42
		-0.425			TDS		[38]			
		-0.46			TDS	0.33	[39]			
Ru	top	-1.66	-1.66	-1.66	TDS	0.20	[40]	-1.89	-1.82	-1.69
Rh	top	-1.5	-1.38	$\approx -1.44$	TDS	0.2-0.25	[41]	-1.89	-1.86	-1.55
		-1.37	-0.77	$\approx -1.07$	TDS	0.25	[42]			
		-1.71			TREELS		[43]			
		-1.40	-1.28	-1.36	He		[44]			
Pd	hollow	-1.30			TDS		[45]	-2.14	-2.09	-1.68
		-1.54	-1.30	$\approx -1.42$	TDS	0.25	[46]			
Ag	top		-0.28		TDS		[47]	-0.16	-0.14	0.18
Ir	top	-1.81	-1.55	$\approx -1.63$	TDS	0.25	[48]	-1.98	-1.94	-1.64
			-1.52			0.33	[49]			
Pt	top	-1.50			TDS	0.25	[50]	-1.70	-1.67	-1.34
		-1.39	-1.22	$\approx -1.33$	LITD	0.25	[51]			
		-1.43	-1.30	$\approx -1.37$	TDS	0.25	[52]			
Au	top		-0.40		TDS		[53]	-0.32	-0.24	0.12

TABLE I: Experimental heats of adsorption for  $\Theta=0$  and 0.25 ML (if available) and the integral heat of adsorption between zero limit and 0.25 ML. Integral heats of adsorption  $H_{\text{ads,int}}$  are compared with our calculated adsorption energies  $E_{\text{ads}}$  at the experimentally observed adsorption sites for the PW91 and RPBE exchange-correlation functionals using two different sets of pseudopotential ( $E_{\text{cut}} = 450$  eV,  $E_{\text{cut}} = 700$  eV, cf. text). TDS - Thermal Desorption Spectroscopy, CAL - Calorimetry method, He - Helium scattering method, LITD - Light Induced Thermal Desorption, SP - SP measurement, TREELS - Time Resolved Electron Energy Loss Spectroscopy.

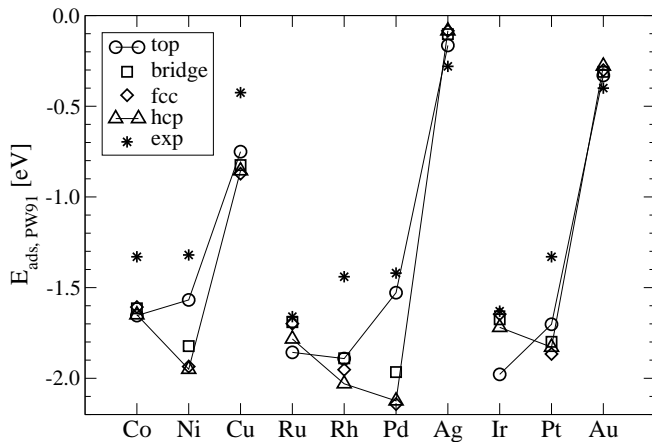


FIG. 5: Calculated CO adsorption energies on TM surfaces for the PW91 exchange-correlation functional and energy cut-off 450 eV. Experimental CO heat of desorption are labelled by the stars (see Table I).

the surface. The tilt with respect to the surface normal is always less than  $2^\circ$ .

The minimum distance between neighboring adsorbates varies in our setup ( $c(2 \times 4)$ ) between 4.3 Å (Co) to 5.1 Å (Au). Therefore direct as well as indirect inter-

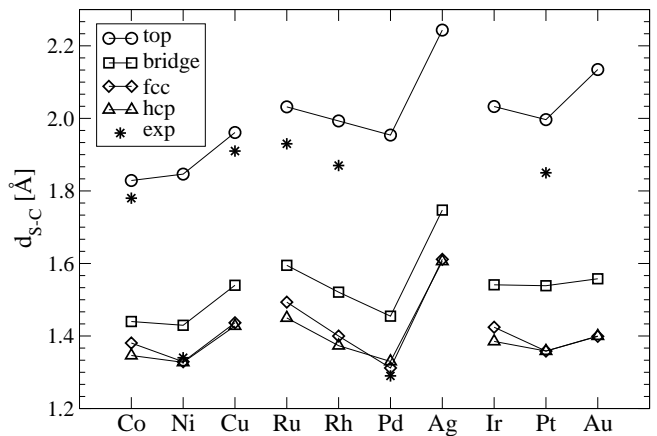


FIG. 6: Calculated heights of the CO adsorbate (surface-C distance) in different adsorption sites on various TM surfaces together with values taken from experimental literature (Table II).

actions can be considered to be small and our calculations probe the low-coverage case.

In response to the adsorption of the CO molecule, the metal atoms in the immediate surrounding move outwards. This effect is quite localized. The buckling is

less pronounced for adsorption in higher coordinated sites ( $\sim 0.1$  Å) and increases for one-fold coordinated CO in an on-top position to  $\sim 0.2$  Å.

The height of the CO molecule above the surface ( $d_{S-C}$ ) is determined by the extension of the metal d-orbitals and (for the higher coordinated sites) by the nearest neighbor distance of the substrate atoms. The greater the extension of the interacting metal orbitals the larger is the distance between the C-atom and the closest metal atom ( $d_{M-C}$ ). Similarly, for a given metal-C distance, the molecule will adsorb at lower height for greater lattice constants. The essential importance of the metal-carbon bond distances for understanding the mechanism of the metal-CO bonding was pointed out earlier [10].

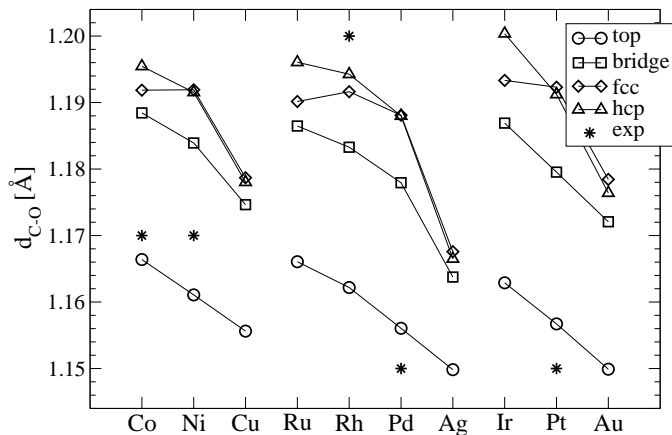


FIG. 7: Calculated C-O bond lengths in top, bridge, fcc and hcp hollow sites on TM surfaces together with experimental values as listed in Table II.

As it was already indicated in the previous studies, a different occupation of the interacting d-band orbitals leads to different values for the  $d_{S-C}$  and  $d_{M-C}$  lengths. In Figs. 6 and 7 the main characteristics of the CO adsorption geometry on TM surfaces are compiled.

When comparing the adsorption geometry, the noble metals behave differently from all other metals. This reflects the completely filled d-band and hence the different bonding mechanism. Adsorption on the noble metals is significantly weaker (see adsorption energies Fig. 5), and consequently the  $d_{S-C}$  and  $d_{M-C}$  lengths are enhanced (see Fig. 6). On the other hand, CO adsorption on the surfaces of TM is stronger and  $d_{S-C}$  (resp.  $d_{M-C}$ ) tends to decrease as the filling of the d-band increases. This trend is more pronounced for 4d than for 5d or 3d metals (for Co and Ni this does not hold for on-top adsorption). For on-top adsorption, the height of the adsorbate increases going from 3d via 4d to 5d elements. The coordination has a strong effect on the CO height: CO in the lower coordinated sites is closer to the surface.

The C-O bond length ( $d_{C-O}$ ) of the free molecule was calculated to be 1.142 Å. On adsorption, the  $d_{C-O}$  length increases with the coordination of the adsorp-

tion site, similarly to  $d_{S-C}$  and  $d_{M-C}$ :  $d_{C-O}$  rises from 1.15 – 1.17 Å for one-fold to 1.17 – 1.20 Å for three-fold coordinates sites. This trend was already stressed in the experimental work of Westerlund et al. [54]. Additionally, the C-O bond is more elongated as the filling of the d-band decreases.

There are many data for the geometrical structure of the CO adsorption on TM from past experiments [55]–[62]. Only for iridium, gold and silver surfaces we are not aware of any experimental literature. A valuable collection of the detailed experimental data for the adsorption of small molecules on the metallic surfaces can be found in the study of Over [3]. A part of the vast data is presented in Table II.

The main difficulty in comparison with experiment (LEED, XPD, EXAFS, ...) is that the estimated error for the C-O bond length ( $\sim \pm 0.05$  Å) is mostly too large, covering the whole interval of all calculated  $d_{C-O}$  values. Although the  $c(2 \times 4)$ -CO structure used in the calculation is not realized on all metallic surfaces, values for  $p(\sqrt{3} \times \sqrt{3})$  and  $p(2 \times 2)$  structures give values in line with our results. This implies that the CO adsorbate-adsorbate interactions at a coverage lower than  $\Theta = \frac{1}{3}$  ML play only a minor role.

### C. Vibrational frequencies

Vibrational frequencies can be measured very accurately using infrared spectroscopy (RAIRS), electron energy loss spectroscopy (EELS) and sum frequency generation (SFG) methods. The dependence of the stretching frequency  $\nu_{C-O}$  on the coordination by the surface atoms has often been used as an indication of the adsorption site. The correlation between the vibrational and electronic properties was analyzed in the paper by Ishi et al. [10] in which a correlation between  $\nu_{C-O}$  and the energy level difference between  $5\tilde{\sigma}$  ( $5\tilde{\sigma}$  character after adsorption) and  $1\tilde{\pi}$  orbitals of the adsorbed CO ( $\Delta(5\tilde{\sigma} - 1\tilde{\pi})$ ) was suggested.

In the following we will focus on two eigenmodes: the M-CO ( $\nu_{M-CO}$ ) and the C-O ( $\nu_{C-O}$ ) stretching frequencies. Our calculated  $\nu_{C-O}$  values are compiled in Fig. 8. For free CO molecules a stretching frequency of  $\nu_{C-O}$  2136  $\text{cm}^{-1}$  was calculated, this value is lowered due to the formation of the bond between the molecule and the metallic surface. The C-O vibrations exhibit the expected strong coordination dependence: CO molecules adsorbed in the lower coordinated sites vibrate faster, typical values for the C-O stretching frequency are 1990–2100  $\text{cm}^{-1}$ , 1830–1880  $\text{cm}^{-1}$ , 1750–1810  $\text{cm}^{-1}$  for carbon monoxide in top, bridge and hollow sites. The stretching frequency for the CO molecule in bridge and hollow sites on noble metals is higher than on the TMs whereas for on-top adsorption the frequencies are almost the same for the noble metals and those of the Pt group.

The dependence of  $\nu_{C-O}$  on the d-band filling of the substrate is also obvious: increased d-band filling raises

Experiment						Theory	
surface	site	$d_{S-C}$ (Å)	$d_{C-O}$ (Å)	$\Theta$ (ML)	ref.	$d_{S-C}^{cal}$ (Å)	$d_{C-O}^{cal}$ (Å)
Co	top	$1.78 \pm 0.06$	$1.17 \pm 0.06$	0.33	[55]	1.83	1.166
Ni	hollow	$1.34 \pm 0.07$	$1.15 \pm 0.07$	0.5	[56]	1.329	1.192
	hollow	$1.29 \pm 0.08$	$1.18 \pm 0.07$	0.5	[56]	1.327	1.192
Cu	top	$1.91 \pm 0.01$		0.33, 0.44	[57]	1.96	1.156
Ru	top	$1.93 \pm 0.04$	$1.10 \pm 0.05$	0.33	[58]	2.03	1.166
Rh	top	$1.87 \pm 0.04$	$1.20 \pm 0.05$	0.33	[59]	1.99	1.162
Pd	hollow	$1.27 \pm 0.04$	$1.14^{+0.14}_{-0.11}$	0.33	[60]	1.31	1.188
	hollow	$1.29 \pm 0.05$	$1.15 \pm 0.04$	0.33	[61]	1.33	1.188
Pt	top	$1.85 \pm 0.10$	$1.15 \pm 0.1$	0.3	[62]	2.00	1.157

TABLE II: Experimental geometrical structures from low energy electron diffraction (LEED) studies of the CO adsorption on TM surfaces together with the values obtained in this study (superscript “cal”). The normal distance between carbon and the TM surface ( $d_{S-C}$ ) and C-O bond length ( $d_{C-O}$ ) at the coverage  $\Theta$  together with corresponding references.

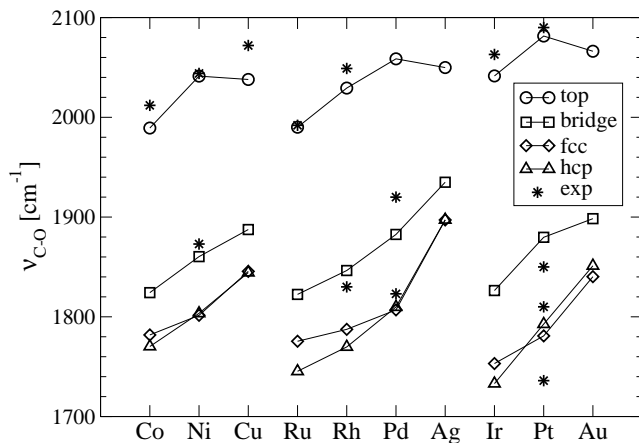


FIG. 8: Calculated C-O stretching frequencies ( $\nu_{C-O}$ ) on closed-packed TM surfaces together with experimental values as listed in Table III. The calculated value of  $\nu_{C-O}$  for the free CO molecule is  $2136 \text{ cm}^{-1}$  compared to the experimental value of  $2145 \text{ cm}^{-1}$ .

$\nu_{C-O}$ ; the correlation is essentially linear. An exception to the rule is CO in on-top sites on noble metals. With decreasing d-band filling the stretching frequencies for the CO adsorbed in the fcc and hcp hollows begin to differ, with the lower  $\nu_{C-O}$  for the hcp sites.

The adsorbate-substrate stretching frequencies  $\nu_{M-CO}$  are compiled in Fig. 9.  $\nu_{M-CO}$  exhibits a similar coordination dependence as  $\nu_{C-O}$ : CO molecules adsorbed in the lower coordinated sites vibrate faster, typical intervals of the  $\nu_{M-CO}$  stretching frequencies on the TM surfaces are  $400\text{--}475 \text{ cm}^{-1}$ ,  $340\text{--}380 \text{ cm}^{-1}$ ,  $300\text{--}350 \text{ cm}^{-1}$  for top, bridge and hollow sites. There is no pronounced correlation with the d-band filling. For noble metals  $\nu_{M-CO}$  lies generally below  $300 \text{ cm}^{-1}$  and there is only a very weak site dependence. Once more, this reflects the weak CO-noble metal bonding. The metal-substrate stretching frequency is particularly low for the Ag surface, consistent with a very low adsorption energy. We have collected available experimental data for  $\nu_{C-O}$  and  $\nu_{M-CO}$

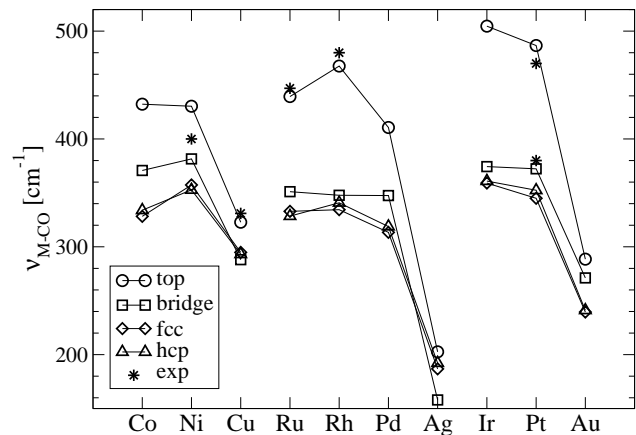


FIG. 9: Calculated M-CO vibrational frequencies ( $\nu_{M-CO}$ ) on closed packed TM surfaces together with experimental values as compiled in Table III.

frequencies in Table III and included them in Fig. 8 and 9. Agreement between the experiment and theory is very good.

As a final remark we emphasize that here only high symmetry sites have been considered. A mixed occupation of different sites or off-symmetry adsorption at higher coverage can significantly increase the CO stretch frequency. As an example we refer to a recent publication on adsorption of CO on the Ni(111) surface presented by Eichler [56].

#### D. Electronic structure

The electronic structure provides deep insight into the interaction between adsorbate and surface. There are many papers which deal with electronic structures and their influence on the trends in binding energy or geometrical structure of the CO molecule on metallic surface [8, 10]. The importance of the interplay between the geometric and the electronic structure in the understanding

Experiment							Theory		
surface	site	$\nu_{M-CO}$ (cm <sup>-1</sup> )	$\nu_{C-O}$ (cm <sup>-1</sup> )	$\Theta$ (ML)	Method	Ref.	$\nu_{M-CO}^{cal}$	$\nu_{C-O}^{cal}$	
Co	top		2012	0.33	RAIRS	[63]	432	1989	
Ni	top		2044	0.25	RAIRS,HREELS	[56]	430	2041	
	hollow	400	1873	0.25	RAIRS,HREELS	[56]	353	1804	
Cu	top	346	2072		RAIRS	[64]	323	2038	
		331	2077	0.33	EELS,RAIRS	[65]	-	-	
			2075	low(0.5L)	RAIRS	[66]	-	-	
Ru	top	445	1980-2080	0.07	EELS	[67]	439	1990	
		447	1990	0.33	RAIRS	[68]	-	-	
			1992	0.25	HREELS	[69]	-	-	
Rh	top		2000	0.33	HREELS	[59]	468	2029	
		480	1990	low	HREELS	[70]	-	-	
			2049	0.2	HREELS	[71]	-	-	
Pd	hollow		1830	0.2	HREELS	[71]	328	1782	
			1848	0.33	RAIRS	[60]	319	1810	
			1823	<0.25	RAIRS	[72]	-	-	
Pd	bridge		1823-1850	<0.33	HREELS	[73]	-	-	
			1920	0.5	RAIRS	[60]	348	1883	
			2137	low(2L)	HREELS	[74]	203	2050	
Ag	top		2063	low(1L)	RAIRS	[48]	505	2041	
			2028-2090	0-0.71ML	RAIRS	[75]	-	-	
			2065	0.25	RAIRS	[76]	-	-	
Pt	top	470	2100	0.24	EELS	[50]	487	2081	
			2090		SFG	[77]	-	-	
		464		0.5	RAIRS	[78]	-	-	
		467	2104	0.5	RAIRS	[79]	-	-	
			2093	0.07	RAIRS	[80]	-	-	
			2095	0.1	RAIRS	[81]	-	-	
			2100	0.25	RAIRS	[82]	-	-	
			380	1850	0.24	EELS	[50]	372	1880
			376		0.5	RAIRS	[78]	-	-
				1855	0.5	RAIRS	[79]	-	-
Pt	hollow		1858	0.07	RAIRS	[80]	-	-	
			1810	0.5	RAIRS	[82]	352	1793	
			1736	0.51	RAIRS	[83]	-	-	

TABLE III: Experimental and calculated metal-CO ( $\nu_{M-CO}$ ) and C-O vibrational frequencies ( $\nu_{C-O}$ ) of CO adsorbed on 3d and 4d TM surfaces. The coverage  $\Theta$  and references to the experimental studies are added. RAIRS - Reflection-Absorption Infra-Red Spectroscopy, (HR)EELS - (High Resolution) Electron Energy Loss Spectra, SFG - Sum Frequency Generation spectroscopy.

of CO adsorption was stressed by Föhlisch et al. [84]. In our analysis we essentially follow the ideas expressed in Refs. [85, 86, 87].

How is CO adsorbed on the TM surface? It is generally assumed that a major part of the CO - metal interaction can be explained in terms of frontier orbitals (the highest occupied molecular orbital (HOMO) and the lowest occupied molecular orbital (LUMO) orbitals). The Blyholder model is based on the donation from the occupied CO-5 $\sigma$  states into empty surface orbitals and the back-donation from occupied surface orbitals to the CO-2 $\pi^*$  orbitals [1].

At this point we can divide the literature into three groups. To the first belong those that agree with the Blyholder model completely [1, 88, 89]. The second group consists of those that agree with Blyholder (in principle), but point out that the Blyholder model ignores the contribution to the bonding from the 4 $\sigma$  and 1 $\pi$  orbitals.

Some consider the model not only oversimplified, but propose another 2 $\pi^*$  resonance model like Gumhalter et al. [90]. And finally to the third group belong those that disagree with the Blyholder model and claim that there is no back-donation to the 2 $\pi^*$  orbital [91].

Although in the experimental study of Nilsson et al. [92], the authors emphasize that an atom-specific look at the CO adsorption could provide insight into the surface chemical bond, we have projected the DOS onto the molecular CO orbitals. The density of states projected onto 1 $\pi$ , 2 $\pi^*$ , 5 $\sigma$  and 4 $\sigma$  molecular orbitals (PDOS) of a CO molecule in top, bridge, hollow sites and a CO molecule far above ( $\sim 4$  Å) the surface is depicted in the Fig 10. The weakly bonded CO molecules on the Au(111) surface already render the general interaction trends. The corresponding analysis of the orbitals of a CO molecule on Pt(111) can also be found in the paper by Kresse et al. [85].



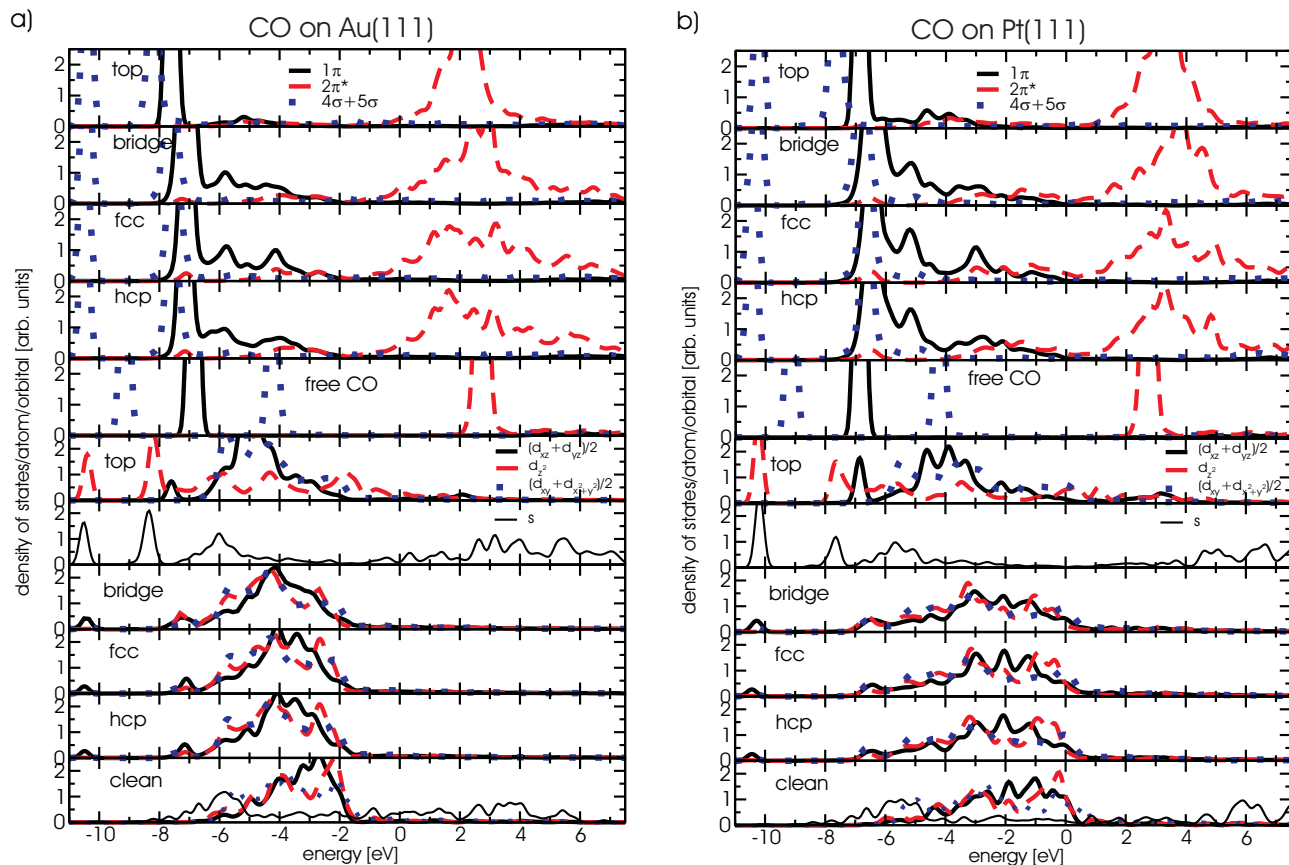


FIG. 10: The projected electronic densities of states (PDOS) for the CO molecule adsorbed in top, bridge, fcc and hcp hollow sites of the Au (a) and Pt (b) surface. While the upper five panels describe the PDOS for various molecular orbitals of the CO molecule, the lower six panels show the PDOS for the substrate atom(s) interacting most with the molecule. The panels labelled 'free CO' and 'clean' describe the noninteracting case for comparison (molecule 4 Å above the surface). The DOS is smoothed by a Gaussian function with a width of 0.2 eV and the Fermi level is located at 0 eV.

There is no principal difference between the Au and Pt DOS. As the CO molecule approaches the surface the localized CO orbitals,  $3\sigma$  (not shown) and  $4\sigma$ , are shifted to lower energies, depending on the coordination between  $\sim 1$  and 3 eV. Since they are fully occupied they play only a minor role in the interaction with the metal, characterized as Pauli repulsion. On the other hand, the  $5\sigma$ ,  $1\pi$  and  $2\pi^*$  peaks broaden and dominate the interaction. Again, the broadening and the shift of the peaks increase with coordination: the higher the coordination - the greater the shift and the broadening. This behavior is more visible for the  $5\sigma$  than for the  $2\pi^*$  peak. The position of the  $5\sigma$  band peak is almost always lower than the  $1\pi$  peak which is shifted by  $\sim 1$  to 3 eV. The  $5\sigma$  band is higher in energy only for on-top adsorption of CO on the Ag(111) surface, which is partially related to the weak interaction. A typical shift for the  $5\sigma$  peak is 3 to 4 eV, depending on the metal CO bond strength. Finally, also the  $2\pi^*$  band broadens with increasing coordination and is therefore partially shifted below the Fermi level ( $E_{\text{Fermi}} = 0$  eV) as shown in Fig 10.

The detailed interaction picture on different sites de-

pends on the symmetry of the surface and adsorbate orbitals. For the top site the major orbital interaction (due to symmetry) is  $5\sigma$  (CO) -  $d_{z^2}$  (metal), whereas for the higher coordinated sites the  $1\pi$  and  $2\pi^*$  CO molecular orbitals are more important, interacting with the  $d_{xz}$  (resp.  $d_{yz}$ ) and in-plane ( $d_{x^2-y^2}$ ,  $d_{xy}$ ) orbitals of the metal atoms. The  $5\sigma$  orbital of the CO orbital adsorbed on-top hybridizes with the  $d_{z^2}$  states of the metallic substrate and shifts to lower energies. The  $d_{z^2}$  states broaden and split into a  $5\sigma - d_{z^2}$  bonding contribution far below the Fermi-level ( $\sim 7.5$  eV) and  $5\sigma - d_{z^2}$  anti-bonding contributions located above the bonding peak and partly even above the Fermi-level. This interaction would be repulsive (Pauli like) if the  $5\sigma - d_{z^2}$  were not pushed partly above the Fermi-level. A  $5\sigma$  depletion (donation from CO to metal) is in accordance with the Blyholder argument of donation of electrons from the adsorbate to the surface [1]. The interaction between the  $5\sigma$  orbitals and the metal s-band is attractive, but depends on the amount of electrons accumulated in the newly created molecular orbitals of the CO-metal system. If we consider a depletion of the  $5\sigma$  orbital, then the interaction with the metallic

s-band becomes more attractive.

The interaction between the  $1\pi$  (resp.  $2\pi^*$ ) orbitals and the substrate is more complex [84]; we can distinguish four contributions: (i) The main part of the  $1\pi$  CO orbital is located at energies around  $\sim -6$  eV. (ii) During the adsorption the peak broadens at the higher energy end up to the Fermi level. This broad state is usually called  $d_{\tilde{\pi}}$  orbital. All the interactions with the  $1\pi$  orbital are located below the Fermi level and have repulsive character [93]. (iii) Furthermore, in the same energy region is a contribution from a partially occupied  $2\pi^*$  orbital which increases with coordination and decreases with the d-band filling (see Fig. 10). This contribution develops into a broad peak for Pt. (iv) Finally, at higher energies ( $\sim 3$  eV) the anti-bonding  $2\pi^*$ - $d_{yz}$ ( $d_{xz}$ ) hybridized orbital is visible.

The later two contributions can be characterized by the fractional occupation of the  $2\tilde{\pi}^*$  orbital, compiled in Table IV. At this point one should remark that our representation of the DOS projected onto molecular orbitals is subject to small inaccuracies not in position, but in amplitude arriving from the projection of the plane-wave components. There exists a tiny hybridization between the molecular  $1\tilde{\pi}$  and  $2\tilde{\pi}^*$  orbitals, therefore the calculated DOS is slightly overestimated at the position of the  $2\tilde{\pi}^*$  for the  $1\tilde{\pi}$  and at the position of the  $1\tilde{\pi}$  for  $2\tilde{\pi}^*$ . This must be considered when calculating the occupation of the  $2\tilde{\pi}^*$  orbital.

Occupation of $2\tilde{\pi}^*$										
site	Co	Ni	Cu	Ru	Rh	Pd	Ag	Ir	Pt	Au
top	16.0	11.5	8.1	11.4	10.8	8.8	5.3	11.4	10.0	6.0
bridge	19.5	14.5	11.1	12.5	11.4	10.5	7.0	11.1	10.1	7.4
fcc	29.9	22.1	16.3	18.5	18.5	18.1	11.7	20.5	19.8	15.0
hcp	29.7	21.6	16.1	19.9	19.5	18.2	11.5	21.4	19.7	14.4

TABLE IV: Fractional occupation of the  $2\tilde{\pi}^*$  orbital for the CO molecule in top, bridge, fcc and hcp sites on the close-packed transition metal surfaces in %.

The occupation of the  $2\tilde{\pi}^*$  orbital increases with coordination, but decreases with d-band filling and also from 3d to the 4d and 5d elements. We can further correlate the site preference between the two competitive (fcc and hcp) hollow sites to the occupation of  $2\tilde{\pi}^*$  orbital. As the occupation of the orbital for the fcc site compared to hcp site increases, the site preference changes from the hcp to the fcc hollow sites. This effect is probably due to a better interaction with the metal atom in the second layer below the hcp site for metals with smaller lattice constants.

### E. Charge density redistribution

In this section, we illustrate the ideas derived in the previous section from the analysis of the DOS by analyzing the charge density and the difference in the charge

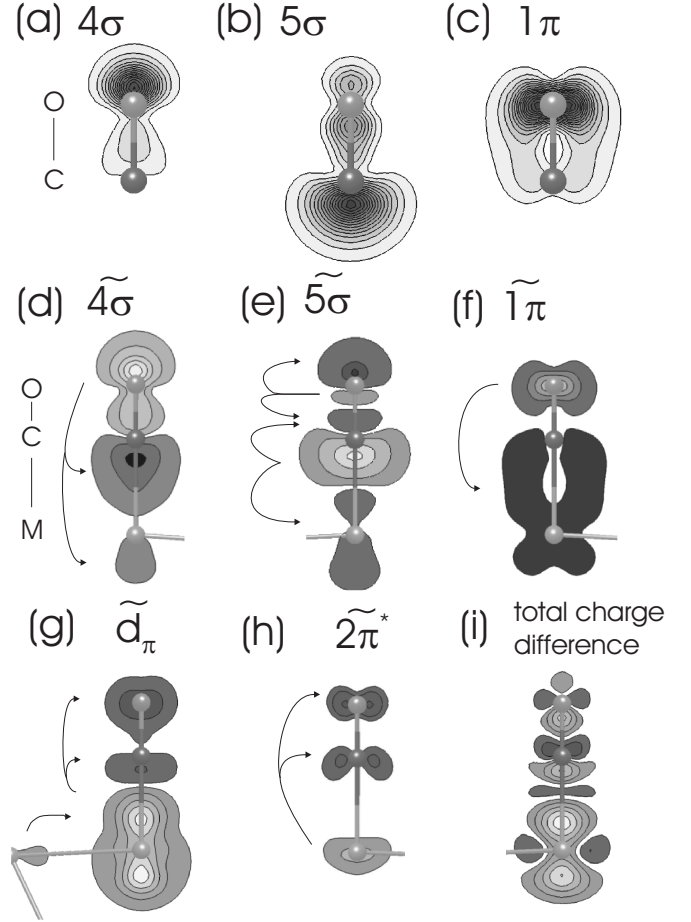


FIG. 11: Charge density of (a)  $4\sigma$ , (b)  $5\sigma$ , (c)  $1\pi$  CO orbitals for the free molecule and the difference ( $\Delta\rho = \rho_{\text{CO+Au(111)}} - \rho_{\text{Au(111)}} - \rho_{\text{CO}}$ ) after the adsorption in the top site of the Au(111) surface (d, e, f). Figures (g) and (h) show the change in the metal charge density due to CO adsorption in the energy interval ( $-5.9$ ,  $-1.0$ ) and just below Fermi level ( $-0.2$ ,  $E_F$ ). The total charge density difference due to adsorption is shown in Fig. (i). Dark regions: charge accumulation, light regions: charge depletion.

density for the molecular orbitals of the CO molecule adsorbed on-top on Au(111) surface as shown in Fig. 11. At first we show the  $4\sigma$ ,  $5\sigma$  and  $1\pi$  orbital-decomposed charge density of the free CO molecule (panels a–c). We can see the accumulation of the charge density for the  $4\sigma$  and  $1\pi$  orbitals around the oxygen atom and for the  $3\sigma$  (not shown) and  $5\sigma$  orbitals on the carbon atom. Fig. 11d, 11e and 11f illustrate what happens to these orbitals after the CO molecule is chemisorbed on-top on the Au(111) surface. Within the  $4\sigma$  orbital charge density moves from the C-O bond and from above the oxygen atom to the region below the carbon (Fig. 11d). Fig. 11e shows redistribution of charge in the  $5\sigma$  molecular orbital: charge is transferred from the side located closer to the metal to the opposite side of the carbon and oxygen atom. This charge transfer is in line with the

experimental observation of a lone pair localized on the oxygen atom as reported in Ref. [92]. There is only little transfer of charge density from the oxygen orbitals with  $p_x/p_y$  character into the metal-carbon bond ( $1\tilde{\pi}$ ). This re-distribution could be related to the slight inaccuracy of the orthogonalization of  $1\tilde{\pi}$  and  $2\tilde{\pi}^*$  orbitals.

The newly formed hybrid states, either by broadening of the  $1\pi$  orbital ( $d_{\tilde{\pi}}$ ) or by occupation of  $2\pi^*$  orbitals is shown in panels g and h. The  $d_{\tilde{\pi}}$  orbital shows a charge transfer from the d-orbitals towards the  $\pi$ -like molecular orbitals. We can even spot a small depletion of charge at the metal atom which is only a 2nd nearest neighbor of the CO, charge which is attracted towards the metal atom interacting with the CO molecule. Furthermore,  $2\tilde{\pi}^*$  states become occupied as can be seen in Fig. 11h. In the panel i, we present the total charge density difference of all states, i.e. the sum of all mentioned charge density redistributions.

Summarizing, we can say that there is a depletion of charge in the substrate out-of-plane d-orbitals and accumulation of charge density in the in-plane d-orbitals of the substrate. The charge density on CO is re-distributed and additionally some charge is transferred into  $2\pi^*$ -like orbitals, which weakens the C-O bond. The establishment of the M-CO bond is reflected by the accumulation of charge between the bonding species.

## V. IMPROVING SITE PREFERENCE

As previously mentioned the calculations for Cu, Rh, Pt surfaces predict a wrong site preference for CO adsorption and the adsorption energies for different adsorption sites on Co, Ag and Au are almost degenerate, so that small changes in the setup (k-points and neglect of surface relaxation) can alter the site preference. Can harder pseudopotentials (lower  $r_{\text{cut}}$  in the pseudopotential generation) or different GGA approaches influence the site preference? In order to shed light onto this question we repeated our calculations performed with the PW91 exchange-correlation functional and cut-off energy  $E_{\text{cut}} = 450$  eV with a harder pseudopotential which requires a higher  $E_{\text{cut}} = 700$  eV and used two different GGA functionals: PW91, RPBE. The use of RPBE is known to result in lower adsorption energies for CO, improving the agreement with experiment in most cases [17] at almost unchanged geometrical structure. The results for RPBE with  $E_{\text{cut}} = 700$  eV (calculated at the optimized PW91 geometry) are presented in Fig. 12.

Switching to the RPBE GGA changes the energetics drastically by  $\sim 0.3$  eV and the values agree well with the experiments for strong chemisorption. On the other hand, the deviation from the experimentally determined adsorption energy increases for weak bonding. For Ag and Au, the RPBE even predicts CO adsorption to be endothermic. Furthermore, the RPBE functional removes the degeneracy of the adsorption sites for Co(0001) and Ag(111) surface and on-top sites become clearly favoured.

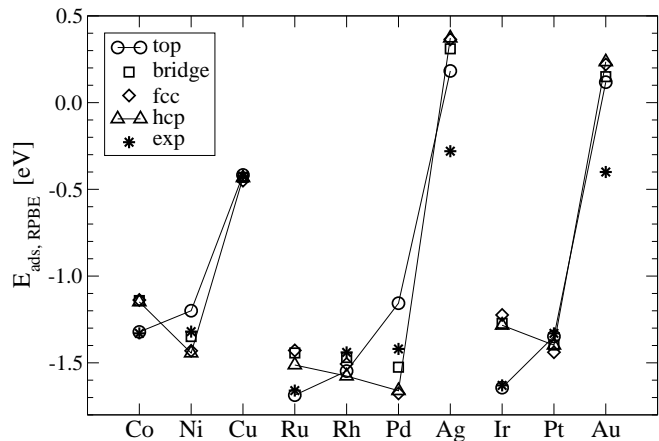


FIG. 12: CO adsorption energies on TM surfaces for the RPBE exchange-correlation functional and energy cut-off 700 eV. Experimental CO heat of desorption are labelled by the stars (see Table I), calculated adsorption energies for top sites are presented with triangles, bridge - squares and fcc hollow - diamonds and hcp sites with circles.

The favoured sites for CO on Rh, Pt, and Cu still contradict the experimental findings. However, in all these cases the corrugation of the potential energy surface is very small compared to metals where CO satisfies the experimental site preference (e.g. Ir and Pd [3]). This also indicates that it is harder for the CO molecule to find the optimal adsorption site on these metals.

To make sure that this large change in  $E_{\text{ads}}$  is not the effect of the  $E_{\text{cut}}$  (larger basis set), but of the different functional, we have recalculated all systems with a harder PW91 pseudopotential which also requires an energy cut-off of  $E_{\text{cut}} = 700$  eV. Besides a small reduction of the adsorption energies (weaker bonding) by about 50 meV the results are identical to those obtained for  $E_{\text{cut}} = 450$  eV.

Summarizing, harder pseudopotentials for C and O lead to a slight decrease of the adsorption energies. The RPBE exchange-correlation functional reduces the adsorption energies by  $\sim 0.3$  eV and improves the differences in adsorption energies for different adsorption sites. However, the site preference remains the same as for the PW91 functional.

## VI. DISCUSSION

In this section, we discuss trends which can be deduced from our results for CO adsorption on closed-packed transition and noble metal surfaces.

### A. Correlations between adsorbate geometry, frequency and adsorption energy

A strong correlation exists between the C-O bond length and the stretching frequency of the CO molecule  $\nu_{C-O}$ . During adsorption the  $2\pi^*$  orbital is partially populated and the C-O bond is weakened. This filling increases from the right to the left in the Periodic Table and with increasing coordination of the adsorption site and hence the CO bond length increases. A weaker and therefore longer C-O bond implies stronger CO-metal bonding and results in lower C-O stretching frequencies. The dependence of  $d_{C-O}$  on the coordination is smallest for the 3d and largest for 4d metals as can be seen in Fig. 7. The trend goes as follows: the higher the reactivity of the surface, the stronger the bonding and population of  $2\pi^*$ -derived orbitals, resulting in a more elongated C-O bond length and a lower stretching frequency.

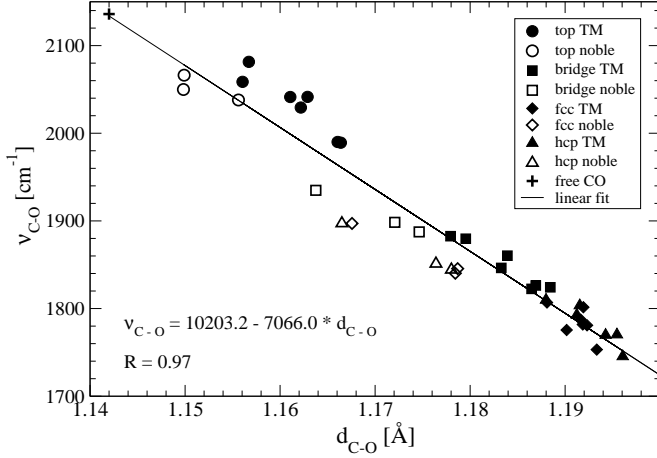


FIG. 13: Correlation between the calculated CO bond length ( $d_{C-O}$ ) and the C-O stretching frequency ( $\nu_{C-O}$ ) for all high-symmetry adsorption sites.

In Fig. 13 the CO stretching frequency is plotted versus the molecular bond length exhibiting a linear relationship between these two properties, which is almost independent of the coordination of the CO molecule. The linear regression fit is characterized by a correlation coefficient of  $R = 0.97$ .

As expected, pronounced stretching of the CO-bond (reflecting a stronger adsorbate-substrate interaction) is accompanied by a decrease of the adsorption height. In Fig. 14 we present this linear relationship between the vibrational frequency  $\nu_{CO}$  and the surface-carbon distance. Remarkably, a trend established by the noble metals alone would be characterized by a much bigger correlation coefficient of  $R = 0.98$  (fit is not shown) compared to the correlation coefficient of  $R = 0.93$  for the complete dataset.

Although we cannot directly relate the height of the molecule on the surface to the adsorption energy it serves

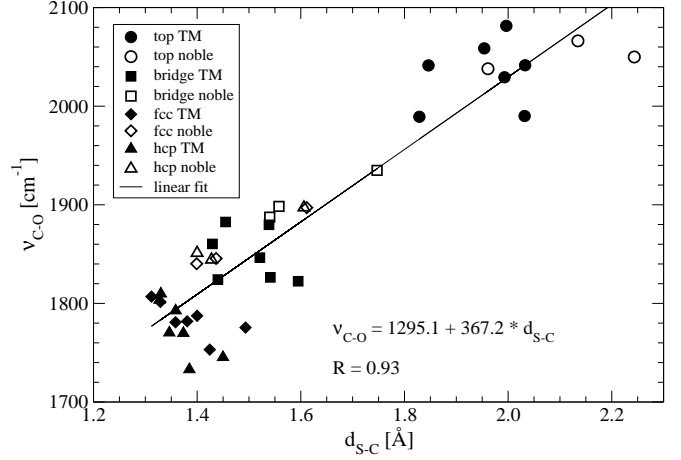


FIG. 14: Correlation between the calculated S-C distance ( $d_{S-C}$ ) and the C-O stretching frequency ( $\nu_{C-O}$ ) for all high-symmetry adsorption sites.

as a rough estimate of the metal-adsorbate interaction. As a consequence of these two linear relationships ( $d_{C-O}$  to  $\nu_{CO}$  and  $d_{S-C}$  to  $d_{C-O}$ ) a similar correlation exists between the  $d_{S-C}$  and  $d_{C-O}$  (Fig. 15). Again, we have divided our dataset into two groups: noble and transition metals and we provide separately a linear fit for each group of our set. Again, the correlation coefficient is higher for noble ( $R_{noble} = 0.98$ ) than for transition metals ( $R_{TM} = 0.93$ ).

Above mentioned linear relationships have an important consequence: if we know one of four measured properties ( $\nu_{C-O}$ ,  $d_{C-O}$ ,  $d_{S-C}$ , or  $d_{M-C}$ ) we can easily estimate all other linearly related properties.

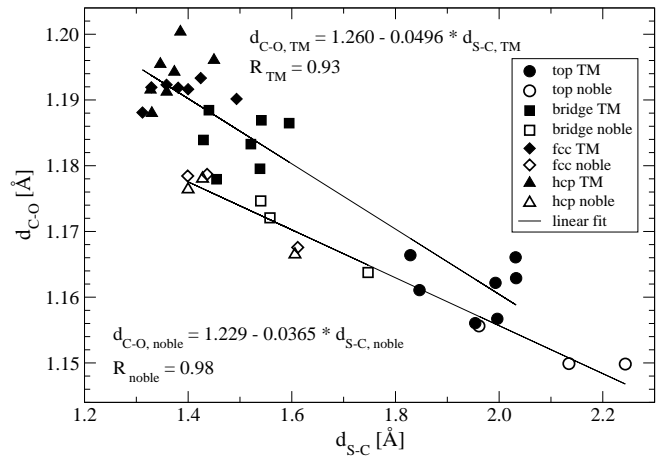


FIG. 15: Correlation between the calculated CO bond length ( $d_{C-O}$ ) and the S-C distance ( $d_{S-C}$ ) for all high-symmetry on-surface sites.

## B. Correlation between the electronic properties of the substrate and adsorption energy

As already mentioned above, one of the most widely discussed models for molecular adsorption on transition metal surfaces is the d-band model of Hammer and Nørskov [8, 9] relating the chemisorption energy to the position of the metallic d-band relative to the molecular orbitals of the adsorbate and to the coupling matrix elements and overlap integrals between the metal d-states and adsorbate states. In a simplified form of the argument, the adsorption energy is related to the d-band position only. This simplified d-band model has recently been examined by Lu et al. [94] for the adsorption of CO, H<sub>2</sub> and ethylene. This analysis led the authors to a critique of the d-band model and of DFT calculations of adsorption energies in general. For CO it was pointed out that the reduction of the adsorption energies with increasing distance of the d-band center from the Fermi energy follows qualitatively the predicted trend, but quantitatively the theoretically predicted dependence is much stronger than what is observed experimentally.

In Fig. 16 we present calculated CO adsorption energies (PW91) with respect to the d-band centers taken from Fig. 4. We can clearly establish a linear relationship between position of the d-band center and the adsorption energy for CO adsorption on noble metals. On the other hand, the values for the transition metals show a large scatter, hence what really determines the trend are the noble metals. It does not mean that there is no relation between the adsorption energy and the d-band center, but it must be corrected for the variation of the coupling matrix elements between different metals, as in the original argument of Hammer and Nørskov [8].

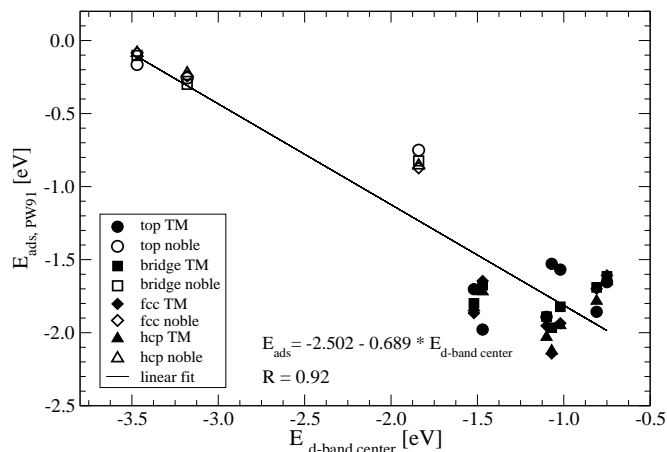


FIG. 16: Correlation between the calculated position of the d-band center (where at least 9.5 electrons are accumulated, see Fig. 4) for all high-symmetry on-surface sites. Empty symbols are for noble metals and full symbols are for transition metals.

## C. Site preference - limitation of DFT

As a by-product of this study the performance of the PW91 functional with different  $E_{\text{cut}}$  (harder potential) and the RPBE functional (well suited for CO and NO adsorption) could be tested on a large number of systems.

A calculation with harder pseudopotential for the same exchange-correlation functional (PW91) leads to small changes in the heat of adsorption which is closer to the experimental value for TMs, but further for noble metals. The site preference does not depend on the basis set for PW91 exchange-correlation functional.

The most important difference between the PW91 and RPBE functional with more accurate pseudopotential ( $E_{\text{cut}} = 700$  eV) is in the absolute value of the of the adsorption energy  $\Delta E_{\text{ads}} \sim 0.3$  eV. Moreover, the difference in the adsorption energy between previously almost degenerate top and hollow adsorption sites is increased (Co, Ag, Au). However, all these changes do not correct the prediction of a wrong adsorption site for Cu, Rh and Pt.

Hence the question “Why does DFT fail in predicting the right adsorption site as well as energy ?” arises. In the past, it has been proposed that a relativistic treatment of transition metals could solve the problem [95, 96, 97]. However, the results presented to support this suggestion are not really convincing, being based on rather thin slabs. Also we note that the work-function of the transition metals is well described and the electronic structure calculations are in good agreement with spectroscopic results. A more promising approach starts from the observation that  $2\pi^*$ -backdonation is the most important contribution to the adsorbate-substrate bond. It is well known that DFT calculations tend to underestimate the HOMO-LUMO gap in CO, facilitating back-donation. Very recently, Kresse et al. [85] have used an LDA+U approach, leading to an increased HOMO-LUMO splitting due to an additional on-site Coulomb repulsion. It was shown that with an increasing HOMO-LUMO gap on Pt(111)  $2\pi^*$  backdonation favouring hollow-adsorption is reduced and site-preference switches to the correct top-site.

Another way to improve the HOMO-LUMO gap is to use hybrid functionals mixing DFT-exchange with exact (Hartree-Fock) exchange: for gas-phase CO the PW91 functional predicts a HOMO-LUMO gap of 6.8 eV, whereas the B3LYP hybrid functionals predicts a splitting of 10.1 eV. However, B3LYP calculations can at the moment only be performed using localized basis sets and small clusters. Very recently Gil et al. [98] have performed a series of cluster-calculations for CO on Pt(111) using both PW91 and B3LYP functionals and slab calculations using PW91. The conclusion is that the B3LYP functional reduces the overestimation of the stability of the hollow site compared to PW91 for a given cluster size. However, the results also show a pronounced cluster-size dependence: for small clusters the preference for the hollow-site is more pronounced than for larger

clusters (the largest cluster considered in this study is Pt<sub>19</sub>). For a comparison of cluster and slab calculations it is concluded that a slab calculation, if performed with a B3LYP functional should favour top adsorption, in agreement with experiment.

Current work is devoted to the extension of the LDA+U approach to other metals and to the investigation of the influence of meta-GGA functionals (incorporating a dependence on the kinetic energy density).

## VII. CONCLUSIONS

The adsorption behavior of the CO molecule on the surfaces of closed-packed late transition metals, namely Co, Ni, Cu, Ru, Rh, Pd, Ag, Ir, Pt, Au has been analyzed using ab-initio DFT methods. To rationalize the trends in the CO adsorption we performed investigations of the geometric structure (metal surface-C and C-O bond length), the electronic structure (projected DOS, charge flow analysis) and the vibrational properties ( $\nu_{\text{C-O}}$  and  $\nu_{\text{M-CO}}$ ). In addition, we examined the influence of different GGAs (PW91, RPBE) on the CO site preference and adsorption energies.

We demonstrate that current DFT slightly overestimates substrate lattice constants (1 to 2%) and underestimates the work-function (by about 0.3 eV). We compared our calculated values for the geometric structure of the adsorbate-substrate complex with experimental data and we find them in very nice agreement. Furthermore, the C-O and M-CO stretching frequencies agree well with

experiments. We illustrate the detailed interaction picture of the CO molecules for different adsorption sites on TM surfaces by means of density of states projected onto molecular CO orbitals and change of the charge density due to adsorption.

Present density functionals overestimate the adsorption energy for sites with high metal coordination compared to sites with low metal coordination. Moreover, the underestimated energy difference between HOMO ( $5\sigma$ ) and LUMO ( $2\pi^*$ ) orbitals contributes to the CO over-binding. DFT fails in predicting the site preference for CO on the Cu (by  $\geq 30$  meV), Rh (by  $\geq 30$  meV), and Pt (by  $\geq 90$  meV) close-packed metal surfaces at 0.25 ML coverage.

Different GGA functionals reduce these discrepancies, but neither harder potentials for CO, nor different GGA functionals correct the results for CO adsorption on these substrates. One should also point out that the adsorption energies calculated using RPBE exchange-correlation functional give results which are much closer to the experimental values for TM surfaces, but predict CO adsorption to be endothermic on the noble metals (Ag and Au).

Recent results have shown that a correct site-preference can be achieved by correcting the HOMO-LUMO gap using techniques beyond DFT. This is after all not entirely surprising, since the analysis demonstrates the importance of the  $2\pi^*$ -backdonation effects, i.e. electron transfer to excited states of the free molecule.

- 
- [1] G. Blyholder, J. Phys. Chem. **68**, 2772 (1964).  
 [2] P. S. Bagus, C. J. Nelin, and C. W. Bauschlicher, Phys. Rev. B **28**, 5423 (1983).  
 [3] H. Over, Prog. Surf. Sci. **58**, 249 (2001).  
 [4] S. Sung and R. Hoffmann, J. Am. Chem. Soc. **107**, 578 (1985).  
 [5] P. Feibelman, B. Hammer, J. Nørskov, F. Wagner, M. Scheffler, and R. Stumpf, J. Phys. Chem. B **108**, 4018 (2001).  
 [6] S. C. Ying, J. R. Smith, and W. Kohn, Phys. Rev. B **11**, 1483 (1975).  
 [7] W. Andreoni and C. M. Varma, Phys. Rev. B **23**, 437 (1981).  
 [8] B. Hammer and J. K. Nørskov, Advances in Catalysis **45**, 71 (2000).  
 [9] J. K. Nørskov, Rep. Prog. Phys. **53**, 1253 (1990).  
 [10] S. Ishi, Y. Ohno, and B. Viswanathan, Surf. Sci. **161**, 349 (1985).  
 [11] <http://cms.mpi.univie.ac.at/vasp/>.  
 [12] G. Kresse and J. Furthmüller, Phys. Rev. B **54**, 11169 (1996).  
 [13] P. Blöchl, Phys. Rev. B **50**, 17953 (1994).  
 [14] G. Kresse and D. Joubert, Phys. Rev. B **59**, 1758 (1999).  
 [15] J. P. Perdew and A. Zunger, Phys. Rev. B **23**, 5048 (1981).  
 [16] J. P. Perdew, J. A. Chevary, S. H. Vosko, K. A. Jackson, M. R. Pederson, D. J. Singh, and C. Fiolhais, Phys. Rev. B **46**, 6671 (1992).  
 [17] B. Hammer, L. B. Hansen, and J. K. Nørskov, Phys. Rev. B **59**, 7413 (1999).  
 [18] A. W. Mantz, J. K. G. Watson, K. N. Rao, D. L. Albritton, A. L. Schmeltekoep, and R. N. Zare, J. Mol. Spectrosc. **39**, 180 (1971).  
 [19] J. D. Cox, D. D. Wangman, and V. A. Medvedev, *CO-DATA Key Values for Thermodynamics* (Hemisphere Publishing Corp., 1984).  
 [20] Landolt-Börnstein, *Strukturdaten der Elemente und intermetallischer Phasen, Neue Serie*, vol. III (Springer, 1971).  
 [21] M. W. Wu and H. Metiu, J. Chem. Phys. **113**, 1177 (2000).  
 [22] M. Mavrikakis, B. Hammer, and J. K. Nørskov, Phys. Rev. Lett. **81**, 2819 (1998).  
 [23] H. B. Michaelson, J. Appl. Phys. **48**, 4729 (1977).  
 [24] F. J. Himpsel, K. Christmann, P. Heimann, D. E. Eastmann, and P. J. Feibelman, Surf. Sci. **115**, L159 (1982).  
 [25] A. Böttcher and H. Niehus, Phys. Rev. B **60**, 14396 (1999).  
 [26] H. A. C. M. Hendrickx, PhD Thesis, Rijksuniversiteit Leiden, The Netherlands (1988).

- [27] R. Fischer, S. Schuppler, N. Fischer, T. Fauster, and W. Steineman, *Phys. Rev. Lett.* **70**, 654 (1993).
- [28] B. E. Nieuwenhuys, *Surf. Sci.* **34**, 317 (1973).
- [29] B. Hammer and J. K. Nørskov, *Surf. Sci.* **343**, 211 (1995).
- [30] B. Hammer, Y. Morikawa, and J. K. Nørskov, *Phys. Rev. Lett.* **76**, 2141 (1996).
- [31] G. Somorjai, *Surf. Sci.* **89**, 496 (1979).
- [32] H. Papp, *Surf. Sci.* **129**, 205 (1983).
- [33] J. Lahtinen, J. Vaari, and K. Kauraala, *Surf. Sci.* **418**, 502 (1988).
- [34] J. T. Stuckless, N. Al-Sarraf, C. Wartnaby, , and D. A. King, *J. Chem. Phys.* **203**, 2202 (1993).
- [35] H. Froitzheim and U. Koehler, *Surf. Sci.* **188**, 70 (1987).
- [36] J. B. Miller, H. R. Siddiqui, S. M. Gates, J. N. Russell Jr., J. T. Yates Jr., J. C. Tully, and M. J. Cardillo, *J. Chem. Phys.* **87**, 6725 (1987).
- [37] S. Vollmer, G. Witte, and C. Woell, *Catal. Lett.* **77**, 97 (2001).
- [38] W. Kirstein, B. Krüeger, and F. Thieme, *Surf. Sci.* **176**, 505 (1986).
- [39] J. Kessler and F. Thieme, *Surf. Sci.* **67**, 405 (1977).
- [40] H. Pfnür and D. Menzel, *J. Chem. Phys.* **79**, 4613 (1983).
- [41] A. B. M. Smedh, M. Borg, R. Nyholm, and J. N. Andersen, *Surf. Sci.* **491**, 115 (2001).
- [42] P. A. Thiel, E. D. Williams, and J. T. Yates, *Surf. Sci.* **84**, 54 (1979).
- [43] D. H. Wei, D. C. Skelton, and S. D. Kevan, *Surf. Sci.* **381**, 49 (1997).
- [44] K. A. Perlinz, T. J. Curtiss, and S. J. Sibener, *J. Chem. Phys.* **95**, 6972 (1991).
- [45] J. Szanyi, W. K. Kuhn, and D. W. Goodman, *J. Vac. Sci. Technol. A* **11**, 1969 (1993).
- [46] X. Guo and J. Yates Jr., *J. Chem. Phys.* **90**, 6761 (1989).
- [47] G. McElhiney, H. Papp, and J. Pritchard, *Surf. Sci.* **54**, 617 (1976).
- [48] M. Sushchikh, J. Lauterbach, and W. H. Weinberg, *J. Vac. Sci. Technol. A* **15**, 1630 (1997).
- [49] C. M. Comrie and W. H. Weinberg, *J. Chem. Phys.* **64**, 250 (1976).
- [50] H. Steininger, S. Lehwald, and H. Ibach, *Surf. Sci.* **123**, 264 (1982).
- [51] E. G. Seebauer, A. C. F. Kong, and L. D. Schmidt, *J. Vac. Sci. Technol.* **5**, 464 (1987).
- [52] G. Ertl, M. Neumann, and K. M. Streit, *Surf. Sci.* **64**, 393 (1977).
- [53] G. S. Elliott and D. R. Miller, in *Proceedings of the 14. International Symposium on Rarefied Gas Dynamics* (Tokyo, 1984), pp. 565, and personal communication.
- [54] L. Westerlund, L. Jönsson, and S. Andersson, *Surf. Sci.* **199**, 109 (1988).
- [55] J. Lahtinen, J. Vaari, K. Kauraala, E. A. Soares, and M. A. Van Hove, *Surf. Sci.* **448**, 269 (2000).
- [56] A. Eichler, *Surf. Sci.* **526**, 332 (2003).
- [57] E. J. Moler, S. A. Kellar, W. R. A. Huff, and Z. Hussain, *Phys. Rev. B* **54**, 10862 (1996).
- [58] H. Over, W. Moritz, and G. Ertl, *Phys. Rev. Lett.* **70**, 315 (1993).
- [59] M. Gierer, A. Barbieri, M. A. Van Hove, and G. A. Somorjai, *Surf. Sci.* **391**, 176 (1997).
- [60] T. Giessel, O. Schaff, C. J. Hirschmugl, V. Fernandez, K. M. Schindler, A. Theobald, S. Bao, R. Lindsay, W. Berndt, A. M. Bradshaw, C. Baddeley, A. F. Lee, R. M. Lambert and D. P. Woodruff, *Surf. Sci.* **406**, 90 (1998).
- [61] H. Ohtani, M. A. Van Hove, and G. A. Somorjai, *Surf. Sci.* **187**, 372 (1987).
- [62] G. S. Blackman, M. L. Xu, D. F. Ogletree, M. A. Van Hove, and G. A. Somorjai, *Surf. Sci.* **61**, 2353 (1988).
- [63] G. A. Beitel, A. Laskov, H. Oosterbeek, and W. W. Kuipers, *J. Phys. Chem.* **100**, 12494 (1996).
- [64] C. J. Hirschmugl, G. P. Williams, F. M. Hoffmann, and Y. J. Chabal, *J. Electron Spectrosc. Relat. Phenom.* **54/55**, 109 (1990).
- [65] R. Raval, S. F. Parker, M. E. Pemble, P. Hollins, J. Pritchard, and M. A. Chester, *Surf. Sci.* **203**, 353 (1988).
- [66] J. K. Eve and E. M. McCash, *Chem. Phys. Lett.* **313**, 575 (1999).
- [67] G. E. Thomas and W. H. Weinberg, *J. Chem. Phys.* **70**, 954 (1979).
- [68] P. Jacob and B. N. J. Person, *Phys. Rev. Lett.* **78**, 3503 (1997).
- [69] P. He, H. Dietrich, and K. Jacobi, *Surf. Sci.* **345**, 241 (1996).
- [70] L. H. Dubois and G. A. Somorjai, *Surf. Sci.* **91**, 514 (1979).
- [71] M. Smedh, A. Beutler, T. Ramsvik, R. Nyholm, M. Borg, J. N. Andersen, R. Duschek, M. Sock, F. P. Netzer, and M. G. Ramsey, *Surf. Sci.* **491**, 99 (2001).
- [72] A. M. Bradshaw and F. M. Hoffmann, *Surf. Sci.* **72**, 513 (1978).
- [73] S. Surnev, M. Sock, M. G. Ramsey, F. P. Netzer, M. Wiklund, M. Borg, and J. N. Andersen, *Surf. Sci.* **470**, 171 (2000).
- [74] W. Hansen, M. Bertolo, and K. Jacobi, *Surf. Sci.* **253**, 1 (1991).
- [75] M. Schick, J. Lauterbach, and W. H. Weinberg, *J. Vac. Sci. Technol. A* **14**, 1448 (1996).
- [76] J. Lauterbach, R. W. Boyle, M. Schick, W. J. Mitchell, B. Meng, and W. H. Weinberg, *Surf. Sci.* **350**, 32 (1996).
- [77] K. Y. Kung, P. Chen, F. Wei, Y. R. Shen, and G. A. Somorjai, *Surf. Sci.* **463**, L627 (2000).
- [78] M. Surman, P. L. Hagans, N. E. Wilson, C. J. Baily, and A. E. Russell, *Surf. Sci.* **511**, L303 (2002).
- [79] E. Schweizer, B. N. J. Persson, M. Tüshaus, D. Hoge, and A. M. Bradshaw, *Surf. Sci.* **213**, 49 (1989).
- [80] J. V. Nekrylova and I. Harrison, *Chem. Phys.* **205**, 37 (1996).
- [81] J. Yoshinobu and M. Kawai, *Surf. Sci.* **363**, 105 (1996).
- [82] B. E. Heyden and A. M. Bradshaw, *Surf. Sci.* **125**, 787 (1983).
- [83] J. V. Nekrylova, C. French, A. N. Artsyukhovich, V. A. Ukraintsev, and I. Harrison, *Surf. Sci. Lett.* **295**, L987 (1993).
- [84] A. Föhlisch, M. Nyberg, J. Hasselström, O. Karis, L. G. M. Pettersson, and A. Nilsson, *Phys. Rev. Lett.* **85**, 3309 (2000).
- [85] G. Kresse, A. Gil, and P. Sautet, *Phys. Rev. B* **68**, 073401 (2003).
- [86] P. S. Bagus and G. Pacchioni, *Surf. Sci.* **278**, 427 (1972).
- [87] R. Hoffmann, *Rev. Mod. Phys.* **60**, 601 (1988).
- [88] F. Illas, S. Zurita, J. Rubio, and A. M. Márquez, *Surf. Sci.* **376**, 279 (1997).
- [89] H. Aizawa and S. Tsuneyuki, *Surf. Sci.* **399**, L364 (1998).
- [90] B. Gumhalter, K. Wandelt, and P. Avouris, *Phys. Rev. B* **37**, 8048 (1988).
- [91] S. Ohnishi and N. Watari, *Phys. Rev. B* **49**, 14619 (1994).
- [92] A. Nilsson, M. Weinelt, T. Wiell, P. Bennich, O. Karis,

- and N. Wassdahl, Phys. Rev. Lett. **78**, 2847 (1997).
- [93] P. Hu, D. A. King, M.-H. Lee, and M. C. Payne, Chem. Phys. Lett. **246**, 73 (1995).
- [94] C. Lu, I. C. Lee, R. I. Masel, A. Wieckowski, and C. Rice, J. Phys. Chem. A **106**, 3084 (2002).
- [95] D. Geschke, T. Baştuğ, T. Jacob, S. Fritzsche, W.-D. Sepp, B. Fricke, S. Varga, and J. Anton, Phys. Rev. B **64**, 235411 (2001).
- [96] I. Grinberg, Y. Yourdshahyan, and A. M. Rappe, J. Chem. Phys. **117**, 2264 (2002).
- [97] R. A. Olsen, P. H. T. Philipsen, and E. J. Baerends, J. Chem. Phys. **119**, 4522 (2003).
- [98] A. Gil, A. Clotet, J. M. Ricart, G. Kresse, M. García-Hernández, N. Rösch, and P. Sautet, Surf. Sci. **530**, 71 (2003).